Pergamon

Polyhedron Vol. 14, No. 13–14, pp. 1731–1740, 1995

0277-5387/95 $9.50+0.00

0277-5387(94)00466-8

MÖSSBAUER AND X-RAY STRUCTURAL STUDIES ON CHLORO(ORGANO)TIN(IV) POLYPYRAZOLYLBORATES

S. CALOGERO* and L. STIEVANO

Dipartimento di Chimica Fisica, Università, I-30123 Venezia, Italy

G. GIOIA LOBBIA and A. CINGOLANI

Dipartimento di Scienze Chimiche, Università, I-62032 Camerino, Italy

and

P. CECCHI

Dipartimento ABAC, Università della Tuscia, I-01100 Viterbo, Italy

and

G. VALLE

Centro dei Biopolimeri del C.N.R., I-35100 Padova, Italy

(*Received* 5 *August* 1994; *accepted* 23 *November* 1994)

Abstract—The ^{119m}Sn Mössbauer parameters at 4.2 K for a series of compounds of general formula $R_nSnCl_{3-n}\cdot L$ [$n = 0$, 1 and 2; R = Me or Ph; L = L^0 hydridotris(1*H*-pyrazol-1-yl)borate, L^1 hydridotris(3-methyl-1*H*-pyrazol-1-yl)borate, L^2 hydridotris(3,5-dimethyl-1*H*-pyrazol-1-yl)borate, or $L^{0'}$ tetrakis(1*H*-pyrazol-1-yl)borate] are reported and discussed. The compounds generally contain a distorted octahedral tin(IV) coordination geometry with one facial *N*-tridentate polypyrazolylborate. The X-ray crystal structures for $SnCl_3\cdot L^0$, $Ph_2SnCl\cdot L^0$ and $Ph_2SnCl\cdot L^2$ confirm these results.

Polypyrazolylborate complexes are still attracting considerable attention.[1] Part of the current interest is due to the possibility of modulating electronic and steric effects by varying the substitution pattern on the ligands.[2]

In the case of organotin(IV) complexes the Lewis acidity of the metal fragment can in general be easily regulated upon substitution of electronegative halogen atom(s) with organyl group(s). Investigations on d^{10} metal complexes such as (organo)tin(IV)[3] or (organo)mercury(II)[4] complexes, containing variously substituted pyrazolylborates, have previously been performed. ^{119}SnNMR data suggested a clear dependence of the chemical shifts on the electronic demand of the tin fragment.[3b] Sound correlations were also obtained with EXAFS measurements.[5]

The series of tin complexes $R_nCl_{3-n}Sn\cdot L$ [$n = 0$, 1 and 2; R = Me or Ph; L = L^0 hydridotris(1*H*-pyrazol-1-yl)borate, L^1 hydridotris(3-methyl-1*H*-pyrazol-1-yl)borate, L^2 hydridotris(3,5-dimethyl-1*H*-pyrazol-1-yl)borate, L^3 hydridotris(3,4,5-Me_3-1*H*-pyrazol-1-yl)borate, $L^{0'}$ tetrakis(1*H*-pyrazol-1-yl)borate, Fig. 1] are particularly suitable as ^{119}Sn nuclide offers the opportunity to take advantage of sensitive techniques such as NMR and Mössbauer spectroscopy. Additional interest in these compounds is conveyed by the known antimutagenic activity displayed by some of them.[6]

Here a representative collection of compounds in the family are examined through Mössbauer spec-

* Author to whom correspondence should be addressed.

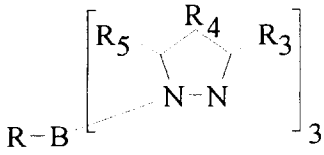

tris(1-*H*-pyrazol-1-yl)borate
or $RB(pz)_3^-$

	Ligand	R	R_3	R_4	R_5
L^0	$HB(pz)_3^-$	H	H	H	H
L^1	$HB(pz)_3^-$	H	Me	H	H
L^2	$HB(pz)_3^-$	H	Me	H	Me
L^3	$HB(pz)_3^-$	H	Me	Me	Me
$L^{0'}$	$pzB(pz)_3^-$	pz	H	H	H

Fig. 1. Identification scheme for the ligands.

troscopy and for three of them the X-ray crystal structures are discussed.

EXPERIMENTAL

The compounds of Table 1 were prepared as previously described.[3-5] Their identity and purity were checked by elemental analysis, melting point determinations, ^1H NMR and IR data. The $Ca^{119m}SnO_3$ Mössbauer source and the absorbers were kept at 4.2 K. A sinusoidal velocity waveform and a proportional detector were used. The spectra have been least squares fitted with sets of equal Lorentzian lines by the program MOS 90. The hyperfine parameters such as isomer shift IS, average linewidth LW, experimental and calculated quadrupole splitting QS, are listed in Table 1. The Mössbauer spectra for the three types of considered stoichiometries are shown in Fig. 2. A minor component attributed to decomposition products has been evidenced in the spectrum of the specimens **14** and **18** of Table 1 (IS 1.07 and 1.19 mm s^{-1}; QS 3.04 and 2.40 mm s^{-1}).

The crystals used for the X-ray determinations were obtained by slow evaporation of a dichloromethane/n-hexane solution for $Ph_2SnCl \cdot L^0$ and $Ph_2SnCl \cdot L^2$, dichloromethane/acetonitrile for $SnCl_3 \cdot L^0$. The evaporation was performed in a glove-box under dry N_2.

Crystal data

$Ph_2SnCl \cdot L^0$ [hydridotris(1*H*-pyrazol-1-yl)borate]diphenylchlorotin(IV)], formula $SnN_6C_{21}BH_{20}Cl$, formula weight $M = 521.2$, orthorhombic, space group $P2_12_12_1$ (n, 19), with $a = 14.302(2)$, $b = 16.721(2)$, $c = 9.041(2)$ Å, $V = 2162.1(6)$ Å^3, $Z = 4$, $D_c = 1.60$ g cm^{-3}, $F(000) = 1040.0$.

$Ph_2SnCl \cdot L^2$[hydridotris(3,5-dimethyl-1-*H*-pyrazol-1-yl)borate]diphenylchlorotin(IV), formula $SnN_6C_{27}BH_{32}Cl$, formula weight $M = 605.3$, monoclinic, space group $P2_1/n$ (n, 14) $a = 10.481(2)$, $b = 19.952(2)$, $c = 13.332(2)$ Å, $\beta = 99.6(2)$, $V = 2749(2)$ Å^3, $Z = 4$, $D_c = 1.46$ g cm^{-3}, $F(000) = 1232.0$.

$SnCl_3 \cdot L^0$ [hydridotris(1*H*-pyrazol-1-yl)borate] trichlorotin(IV), formula $SnN_6C_9BH_{10}Cl_3$, formula weight $M = 438.1$, trigonal, space group $P\bar{3}$ (n, 147), with $a = b = 11.478(2)$, $c = 7.999(1)$ Å, $\gamma = 120°$, $V = 912.6(6)$ Å^3, $Z = 2$, $D_c = 1.59$ g cm^{-3}, $F(000) = 424.0$.

Intensity data were collected at room temperature with a Philips PW 1100 diffractometer by using Mo-K_α radiation in the range $4.9° < 2\theta < 54.7°$ and 2112 independent reflections were observed for $Ph_2SnCl \cdot L^0$ [$4.1° < 2\theta < 56.0°$ and 3765 for $Ph_2SnCl \cdot L^2$; $4.1° < 2\theta < 50.0°$ and 1837 for $SnCl_3 \cdot L^0$]; 1676 reflections with $F > 3\sigma(F)$ for $Ph_2SnCl \cdot L^0$ and 3051 for $Ph_2SnCl \cdot L^2$ [950 for $SnCl_3 \cdot L^0$ with $F > 5\sigma(F)$] were used in the structure analysis. The atoms B, N, Cl, and C were located by three-dimensional Fourier syntheses. Blocked full-matrix least-squares refinement on F was computed and the function $\Sigma w[|F_o| - |F_c|]^2$ minimized. The non-hydrogen atoms were refined anistropically. The positions of the hydrogen atoms were calculated but not refined.

In $SnCl_3 \cdot L^0$ it has been observed a residual electronic density, around the inversion centre, due to the atoms statistically disordered of the acetonitrile, the crystallization solvent. Being interested mostly in the coordination tin(IV) environments, this residual has not been further considered. The final R values were 0.034 (R_w 0.033) for $Ph_2SnCl \cdot L^0$, 0.026 (R_w 0.028) for $Ph_2SnCl \cdot L^2$ and 0.073 (R_w 0.081) for $SnCl_3 \cdot L^0$.

The structures of $Ph_2SnCl \cdot L^0$, $Ph_2SnCl \cdot L^2$ and $SnCl_3 \cdot L^0$ are represented in the ORTEP plot of Fig. 3, together with the numbering scheme. Selected bond distances and angles are in Tables 2–4. The final atomic coordinates, the anisotropic thermal parameters and the structural factors have been deposited with the Editor.*

* Atomic coordinates have also been deposited with Cambridge Crystallographic Data Centre.

Table 1. ^{119m}Sn Mössbauer parameters at 4.2 K

No.	Sample[a]	IS[b,c]	LW[c]	QS[c]	QS calc.[c,d]
1	$SnCl_3 \cdot L^0$	0.16	1.02	0.53	>0
2[e]	$SnCl_3 \cdot L^1$	0.24	0.90	0.25	>0
3	$SnCl_3 \cdot L^2$	0.23	1.05	0.39	>0
4	$SnCl_3 \cdot L^{0\prime}$	0.29	1.12	0.31	>0
5	$MeSnCl_2 \cdot L^0$	0.71	0.94	1.75	+2.06
6[e]	$MeSnCl_2 \cdot L^1$	0.72	0.83	1.73	+2.06
7	$MeSnCl_2 \cdot L^2$	0.71	0.89	1.73	+2.06
8	$MeSnCl_2 \cdot L^{0\prime}$	0.75	0.83	1.92	+2.06
9	$PhSnCl_2 \cdot L^0$	0.65	0.99	1.73	+1.90
10[e]	$PhSnCl_2 \cdot L^1$	0.67	0.83	1.52	+1.90
11	$PhSnCl_2L^2$	0.65	0.95	1.57	+1.90
12	$Me_2SnCl \cdot L^0$	0.88	0.85	2.32	−2.06
13[e]	$Me_2SnCl \cdot L^1$	0.88	0.84	2.26	−2.06
14	$Me_2SnCl \cdot L^2$	0.87	0.98	2.23	−2.06
15	$Ph_2SnCl \cdot L^0$	0.80	1.05	2.03	−1.90
16[e]	$Ph_2SnCl \cdot L^1$	0.83	0.85	2.13	−1.90
17	$Ph_2SnCl \cdot L^2$	0.85	1.05	2.03	−1.90
18	$Ph_2SnCl \cdot L^{0\prime}$	0.77	0.90	2.02	−1.90
19[e]	$(CH_2{=}CH)_2SnCl \cdot L^1$	0.78	0.90	1.99	−2.06
20	$Me_2SnCl \cdot L^{0\prime}$	0.88	0.95	3.31	+2.91[f]

[a] $L = L^0$ hydridotris(1*H*-pyrazol-1-yl)borate, L^1 hydridotris(3-methyl-1*H*-pyrazol-1-yl)borate, L^2 hydridotris(3,5-dimethyl-1*H*-pyrazol-1-yl)borate, or $L^{0\prime}$ tetrakis(1*H*-pyrazol-1-yl)borate.

[b] The shifts are relative to SnO_2.

[c] In mm s^{-1}.

[d] Calculated assuming a regular octahedral geometry and the literature[11] partial quadrupole splittings, in mm s^{-1}, $Cl = 0.00$, $Me = -1.03$, $Ph = -0.95$ together with the working approximations of -0.04 mm s^{-1} (i.e. the value of $\frac{1}{2}$phen as bridging ligand) for all the pyrazolate-type ligands (1/3L). The calculated e.f.g. components are: $V_{xx} = V_{yy} = V_{zz} = 0$ for $SnCl_3 \cdot L$; $V_{xx} = V_{yy} = -R + Cl$, $V_{zz} = 2R - 2Cl$ for $RSnCl_2 \cdot L$; $V_{xx} = V_{yy} = R - Cl$, $V_{zz} = -2R + 2Cl$ for $R_2SnCl \cdot L$.

[e] From ref. 3b.

[f] Calculated for a regular tbp geometry (equatorial Mes).

RESULTS AND DISCUSSION

X-ray crystallographic structures

The compound $Ph_2SnCl \cdot L^0$, shown in Fig. 3(a), consists of covalent molecules in which a distorted octahedral coordination geometry is present. The tin(IV) bond lengths range from 2.155 to 2.445 Å and the bond angles from 76.1 to 103.9°. Details of bond distances and angles are in Table 2. The tin atom is slightly out of the coordination plane N(2), N(3), C(10) and C(16). The molecule is discrete since the absence of relevant intermolecular contacts within 4 Å. The least-squares pyrazolate and phenyl rings are practically planar. The dihedral angles formed by these planes are reported in Table 5. As expected the largest isotropic thermal parameters are exhibited from the atoms farthest from the tin coordination site, i.e. the atoms C(12)···C(14) and C(18)···C(20) of the phenyl groups and from the atoms C(2), C(5) and C(8) of the pyrazole groups.

The discrete compound $Ph_2SnCl \cdot L^2$, shown in Fig. 3(b), is similar to $Ph_2SnCl \cdot L^0$ (Table 3). The phenyl ring containing the atoms C(16) and C(21) deviates somewhat from the planarity, whereas the remaining phenyl and pyrazolate rings are planar. The dihedral angles formed by these

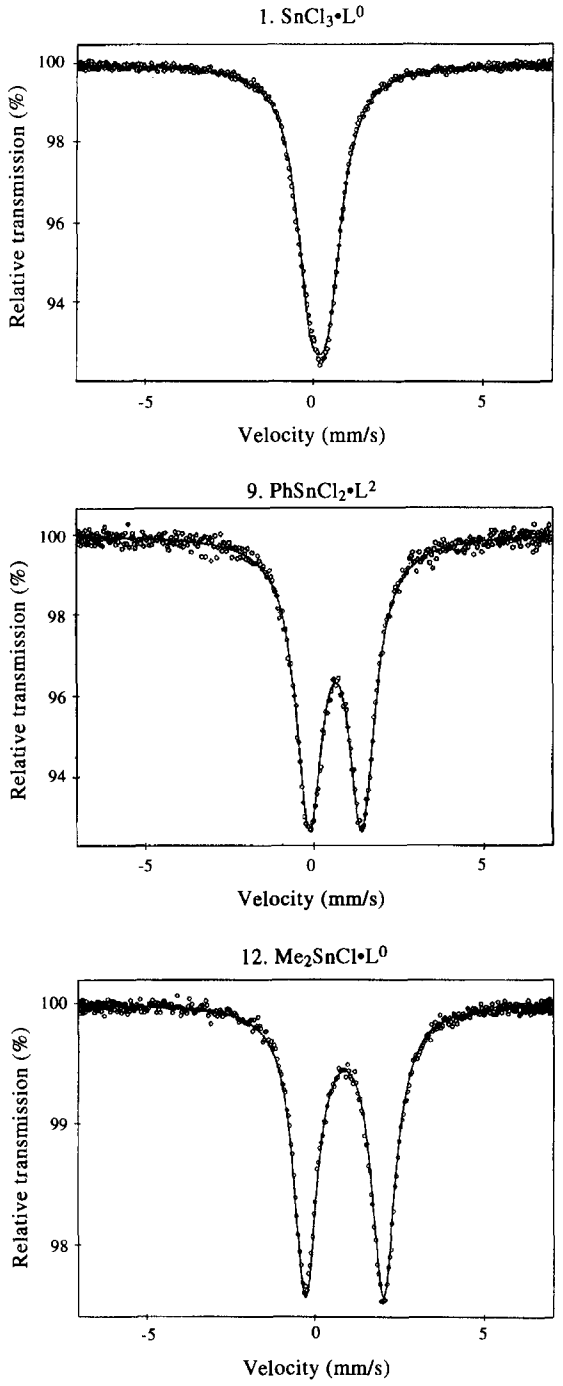

Fig. 2. Mössbauer spectra at 4.2 K for **1** $SnCl_3 \cdot L^0$, **9** $PhSnCl_2 \cdot L^2$ and **12** $Me_2SnCl \cdot L^0$.

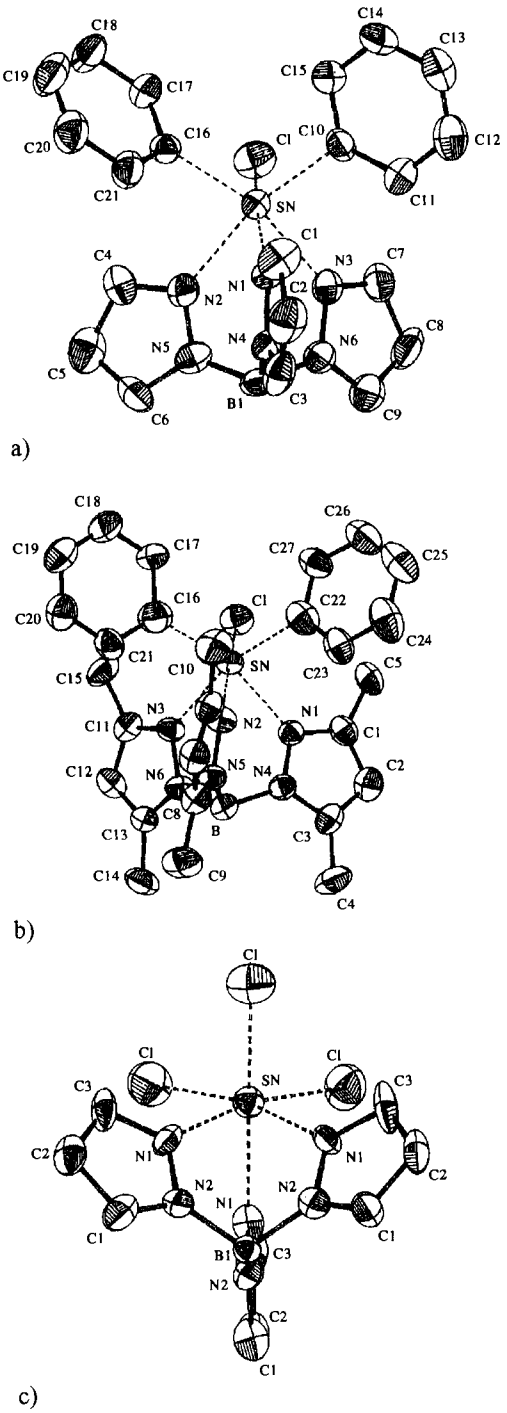

Fig. 3. ORTEP views for: (a) $Ph_2SnCl \cdot L^0$, (b) $Ph_2SnCl \cdot L^2$ and (c) $SnCl_3$ L^0.

least-squared planes are reported in Table 5. The largest isotropic thermal parameters are shown from the methyl atoms C(4), C(9) and C(14) [the farthest from the phenyl atoms C(18), C(19), C(24), C(25) and C(26)]. The smallest isotropic thermal values are shown from the methyls close to the phenyl atoms C(21) and C(24). The packing of the molecules $Ph_2SnCl \cdot L^2$ in the crystal is determined by normal van der Waals contacts.

The covalent compound $SnCl_3 \cdot L^0$, shown in Fig. 3(c), contains discrete molecular unities. The closest contact between a chloride from $SnCl_3 \cdot L^0$ and a nitrogen atom of the acetonitrile is at 3.40(6) Å. As shown in Table 4 the geometry around the tin atom is that of a distorted octahedron with N—Sn—N

Table 2. Selected bond lengths (Å) and angles (°) for $Ph_2SnCl \cdot L^0$

Sn—Cl	2.445(3)	Sn—N(1)	2.271(7)
Sn—N(2)	2.281(7)	Sn—N(3)	2.303(6)
Sn—C(10)	2.155(8)	Sn—C(16)	2.174(8)
N(1)—N(4)	1.36(1)	N(1)—C(1)	1.33(1)
N(2)—N(5)	1.341(9)	N(2)—C(4)	1.32(1)
N(3)—N(6)	1.38(1)	N(3)—C(7)	1.31(1)
N(4)—B	1.55(1)	N(4)—C(3)	1.34(1)
N(5)—B	1.53(1)	N(5)—C(6)	1.35(1)
N(6)—B	1.53(1)	N(6)—C(9)	1.34(1)
C(1)—C(2)	1.37(1)	C(2)—C(3)	1.34(1)
C(4)—C(5)	1.37(1)	C(5)—C(6)	1.35(1)
C(7)—C(8)	1.38(1)	C(8)—C(9)	1.35(2)
C(10)—C(11)	1.39(1)	C(10)—C(15)	1.38(1)
C(11)—C(12)	1.37(2)	C(12)—C(13)	1.37(2)
C(13)—C(14)	1.36(2)	C(14)—C(15)	1.40(2)
C(16)—C(17)	1.39(1)	C(16)—C(21)	1.38(1)
C(17)—C(18)	1.37(1)	C(18)—C(19)	1.37(2)
C(19)—C(20)	1.38(2)	C(20)—C(21)	1.38(1)

C(10)—Sn—C(16)	103.9(3)	N(3)—Sn—C(16)	163.1(3)
N(3)—Sn—C(10)	92.4(3)	N(2)—Sn—C(16)	87.0(3)
N(2)—Sn—C(10)	164.3(3)	N(2)—Sn—N(3)	76.1(2)
N(1)—Sn—C(16)	97.7(3)	N(1)—Sn—C(10)	87.7(3)
N(1)—Sn—N(3)	78.4(3)	N(1)—Sn—N(2)	79.6(2)
Cl—Sn—C(16)	96.32(2)	Cl—Sn—C(10)	99.5(2)
Cl—Sn—N(3)	85.1(2)	Cl—Sn—N(2)	90.3(2)
Cl—Sn—N(1)	162.3(2)	Sn—N(1)—C(1)	130.4(6)
Sn—N(1)—N(4)	124.2(5)	N(4)—N(1)—C(1)	105.3(7)
Sn—N(2)—C(4)	128.5(5)	Sn—N(2)—N(5)	124.4(5)
N(5)—N(2)—C(4)	106.5(7)	Sn—N(3)—C(7)	131.2(6)
Sn—N(3)—N(6)	122.5(5)	N(6)—N(3)—C(7)	106.3(7)
N(1)—N(4)—B	120.0(6)	N(1)—N(4)—C(3)	108.9(7)
C(3)—N(4)—B	130.6(7)	N(2)—N(5)—B	120.6(7)
N(2)—N(5)—C(6)	109.1(7)	C(6)—N(5)—B	130.2(8)
N(3)—N(6)—B	120.5(7)	N(3)—N(6)—C(9)	107.7(7)
C(9)—N(6)—B	131.6(8)	N(1)—C(1)—C(2)	111.3(8)
C(1)—C(2)—C(3)	105.0(9)	N(4)—C(3)—C(2)	109.5(8)
N(2)—C(4)—C(5)	111.1(8)	C(4)—C(5)—C(6)	104.7(9)
N(5)—C(6)—C(5)	108.6(8)	N(3)—C(7)—C(8)	111.7(8)
C(7)—C(8)—C(9)	104.0(8)	N(6)—C(9)—C(8)	110.2(9)
Sn—C(10)—C(15)	117.9(6)	Sn—C(10)—C(11)	123.7(6)
C(11)—C(10)—C(15)	117.9(8)	C(10)—C(11)—C(12)	121.2(8)
C(11)—C(12)—C(13)	120(1)	C(12)—C(13)—C(14)	120(1)
C(13)—C(14)—C(15)	120(1)	C(10)—C(15)—C(14)	120.5(8)
Sn—C(16)—C(21)	122.3(6)	Sn—C(16)—C(17)	119.6(6)
C(17)—C(16)—C(21)	118.1(8)	C(16)—C(17)—C(18)	121.5(9)
C(17)—C(18)—C(19)	120.1(9)	C(18)—C(19)—C(20)	119(1)
C(19)—C(20)—C(21)	121(1)	C(16)—C(21)—C(20)	120.1(9)
N(5)—B—N(6)	108.3(7)	N(4)—B—N(6)	107.3(8)
N(4)—B—N(5)	108.6(8)		

and Cl—Sn—Cl angles 81.6(3)° and 98.3(1)°, respectively. Selected bond lengths and angles for the above reported structures, together with others for similar tin(IV) tris(pyrazolyl)borates[7] are reported in Table 6.[8,9] Data are sufficiently comparable although the principal effects cannot be clearly attributed to either Sn-bonded groups or ligand's substitution pattern within this yet incomplete set of crystal structures.

In the following discussion the symbol Δ* refers

Table 3. Selected bond lengths (Å) and angles (°) for $Ph_2SnCl \cdot L^2$

Sn—Cl	2.456(1)	Sn—N(1)	2.294(4)
Sn—N(2)	2.285(3)	Sn—N(3)	2.306(4)
Sn—C(16)	2.162(5)	Sn—C(22)	2.174(4)
N(1)—N(4)	1.368(4)	N(1)—C(1)	1.343(5)
N(2)—N(5)	1.373(5)	N(2)—C(6)	1.339(5)
N(3)—N(6)	1.378(4)	N(3)—C(11)	1.343(5)
N(4)—B	1.535(5)	N(4)—C(3)	1.346(5)
N(5)—B	1.525(5)	N(5)—C(8)	1.340(5)
N(6)—B	1.540(5)	N(6)—C(13)	1.338(5)
C(1)—C(2)	1.372(6)	C(1)—C(5)	1.491(6)
C(2)—C(3)	1.360(6)	C(3)—C(4)	1.498(6)
C(6)—C(7)	1.381(6)	C(6)—C(10)	1.504(7)
C(7)—C(8)	1.360(6)	C(8)—C(9)	1.499(7)
C(11)—C(12)	1.389(6)	C(11)—C(15)	1.488(7)
C(12)—C(13)	1.358(6)	C(13)—C(14)	1.500(8)
C(16)—C(17)	1.387(6)	C(16)—C(21)	1.387(6)
C(17)—C(18)	1.382(6)	C(18)—C(19)	1.372(8)
C(19)—C(20)	1.366(8)	C(20)—C(21)	1.386(7)
C(22)—C(23)	1.384(6)	C(22)—C(27)	1.395(7)
C(23)—C(24)	1.388(7)	C(24)—C(25)	1.39(1)
C(25)—C(26)	1.360(9)	C(26)—C(27)	1.389(8)

C(16)—Sn—C(22)	107.2(2)	N(3)—Sn—C(22)	163.6(2)
N(3)—Sn—C(16)	88.3(2)	N(2)—Sn—C(22)	92.8(2)
N(2)—Sn—C(16)	89.5(1)	N(2)—Sn—N(3)	82.0(2)
N(1)—Sn—C(22)	86.5(2)	N(1)—Sn—C(16)	163.6(2)
N(1)—Sn—N(3)	77.4(2)	N(1)—Sn—N(2)	80.9(1)
Cl—Sn—C(22)	95.7(2)	Cl—Sn—C(16)	96.7(1)
Cl—Sn—N(3)	87.4(1)	Cl—Sn—N(2)	167.5(1)
Cl—Sn—N(1)	90.5(1)	Sn—N(1)—C(1)	131.8(8)
Sn—N(1)—N(4)	119.8(3)	Sn—N(2)—N(5)	120.6(2)
Sn—N(2)—C(6)	130.9(3)	N(4)—N(1)—C(1)	106.9(3)
N(5)—N(2)—C(6)	106.7(3)	Sn—N(3)—C(11)	132.5(3)
Sn—N(3)—N(6)	120.3(3)	N(6)—N(3)—C(11)	106.9(4)
N(1)—N(4)—C(3)	108.4(4)	N(1)—N(4)—B	120.3(3)
B—N(4)—C(3)	130.5(4)	N(2)—N(5)—C(8)	108.9(3)
N(2)—N(5)—B	120.0(3)	B—N(5)—C(8)	131.0(4)
N(3)—N(6)—C(13)	109.3(3)	N(3)—N(6)—B	120.4(4)
B—N(6)—C(13)	130.3(3)	N(5)—B—N(6)	109.4(3)
N(4)—B—N(6)	108.2(4)	N(4)—B—N(5)	109.8(6)
N(1)—C(1)—C(5)	124.0(4)	N(1)—C(1)—C(2)	109.2(5)
C(2)—C(1)—C(5)	126.8(5)	C(1)—C(2)—C(3)	106.8(4)
N(4)—C(3)—C(2)	108.1(4)	C(2)—C(3)—C(4)	129.9(5)
N(4)—C(3)—C(4)	121.9(5)	N(2)—C(6)—C(10)	122.2(4)
N(2)—C(6)—C(7)	109.5(4)	C(7)—C(6)—C(10)	128.4(4)
C(6)—C(7)—C(8)	106.2(4)	N(5)—C(8)—C(7)	108.7(4)
C(7)—C(8)—C(9)	129.6(4)	N(5)—C(8)—C(9)	121.7(4)
N(3)—C(11)—C(15)	123.8(5)	N(3)—C(11)—C(12)	108.5(4)
C(12)—C(11)—C(15)	127.6(6)	C(11)—C(12)—C(13)	107.0(5)
N(6)—C(13)—C(12)	108.3(5)	C(12)—C(13)—C(14)	130.0(6)
N(6)—C(13)—C(14)	121.7(4)	Sn—C(16)—C(21)	122.1(3)
Sn—C(16)—C(17)	120.4(4)	C(17)—C(16)—C(21)	117.5(4)
C(16)—C(17)—C(18)	121.0(6)	C(17)—C(18)—C(19)	120.3(5)
C(18)—C(19)—C(20)	119.8(6)	C(19)—C(20)—C(21)	119.9(6)
C(16)—C(21)—C(20)	121.4(4)	Sn—C(22)—C(27)	121.2(4)
Sn—C(22)—C(23)	120.6(5)	C(23)—C(22)—C(27)	118.0(6)
C(22)—C(23)—C(24)	121.7(5)	C(23)—C(24)—C(25)	119.1(6)
C(24)—C(25)—C(26)	120.0(8)	C(25)—C(26)—C(27)	121.0(7)
C(22)—C(27)—C(26)	120.2(5)		

Table 4. Selected bond lengths (Å) and angles (°) for $SnCl_3 \cdot L^0$

Sn—Cl	2.376(3)	Sn—N(1)	2.234(7)
N(1)—N(2)	1.37(1)	N(1)—C(3)	1.30(1)
N(2)—C(1)	1.30(1)	N(2)—B	1.551(8)
C(1)—C(2)	1.37(1)	C(2)—C(3)	1.41(2)
Cl—Sn—N(1)	167.9(2)	Sn—N(1)—C(3)	131.3(8)
Sn—N(1)—N(2)	121.4(6)	N(2)—N(1)—C(3)	107.1(8)
N(1)—N(2)—B	119.5(6)	N(1)—N(2)—C(1)	108.2(7)
C(1)—N(2)—B	132.3(7)	N(2)—C(1)—C(2)	112(1)
C(1)—C(2)—C(3)	102(1)	N(1)—C(3)—C(2)	111(1)
N(1)—Sn—N′(1)	81.6(2)	N(2)—B—N′(2)	109.0(3)
Cl—Sn—Cl′	98.5(2)		

Table 5. Dihedral angles (°) formed by least-squared fitted planes

Plane	$Ph_2SnCl \cdot L^0$ Plane	Angle	Plane	$Ph_2SnCl \cdot L^2$ Plane	Angle
C(10)...C(15)	C(16)...C(21)	80.2(3)	C(16)...C(21)	C(22)...C(27)	58.7(2)
C(10)...C(15)	N(1)N(4)...C(3)	55.2(3)	C(16)...C(21)	N(1)N(4)...C(3)	8.6(2)
C(10)...C(15)	N(2)N(5)...C(6)	21.4(3)	C(16)...C(21)	N(2)N(5)...C(8)	53.0(2)
C(10)...C(15)	N(3)N(6)...C(9)	64.4(3)	C(16)...C(21)	N(3)N(6)...C(13)	68.7(2)
C(16)...C(21)	N(1)N(4)...C(3)	62.3(3)	C(22)...C(27)	N(1)N(4)...C(3)	52.5(2)
C(16)...C(21)	N(2)N(5)...C(6)	64.7(3)	C(22)...C(27)	N(2)N(5)...C(8)	68.3(2)
C(16)...C(21)	N(3)N(6)...C(9)	27.2(3)	C(22)...C(27)	N(3)N(6)...C(13)	22.7(2)
N(1)N(4)...C(3)	N(2)N(5)...C(6)	58.7(4)	N(1)N(4)...C(3)	N(2)N(5)...C(8)	59.6(2)
N(1)N(4)...C(3)	N(3)N(6)...C(9)	64.1(4)	N(1)N(4)...C(3)	N(3)N(6)...C(13)	65.0(2)
N(2)N(5)...C(6)	N(3)N(6)...C(9)	57.2(3)	N(2)N(5)...C(8)	N(3)N(6)...C(13)	61.2(2)

Table 6. Selected bond lengths (Å) and angles (°) for tin(IV) tris(pyrazolyl)borates

	$Ph_2SnCL \cdot L^0$ **a**[a]	$Ph_2SnCl \cdot L^2$ **b**[a]	$R^b SnCl2 \cdot L^0$ Ref. 7	$PhSnCl_2 \cdot L^1$ Ref. 3b	$MeSnCl_2 \cdot L^3$ Ref. 8[c]	$SnCl_3 \cdot L^0$ **c**[a]	$SnCl_3 \cdot L^2$ Ref. 9
Sn—C	2.168	2.164	2.140	2.228	2.244	—	—
Sn—N	2.285	2.296	2.218	2.249	2.242	2.234	2.198
Sn—Cl	2.445	2.456	2.428	2.429	2.438	2.376	2.382
N—Sn—N	78.0	80.1	80.3	81.6	82.0	81.6	83.9
N—B—N	108.1	109.1	106.4	109.6	109.1	109.0	109.4
C—Sn—C	103.9	107.2	—	—	—	—	—
C—Sn—Cl	97.9	96.2	97.8	96.5	96.5	—	—
Cl—Sn—Cl	—	—	94.3	93.8	94.5	98.5	93.6

[a] This paper.
[b] R = $CH_2CH_2CO_2Me$.
[c] L^3 = hydridotris(3,4,5-trimethyl-1*H*-pyrazol-1-yl)borate.

to differences between one distance or angle (if a set of values is present the average one is considered) in $Ph_2SnCl \cdot L^2$ (**b**) and $Ph_2SnCl \cdot L^0$ (**a**). Analogously Δ^{**} is for the couple $SnCl_3 \cdot L^2$ (ref. 7) and $SnCl_3 \cdot L^0$ (**c**).

The structures **a** and **b** offer the opportunity to compare the ligand's effects in that the organotin moiety is identical. The phenyl rings show a relative rotation in **a**. Indeed the torsion angles C(15)C(10)C(16)C(17) and C(11)C(10)C(16)C(21) are 40.3° and 37.1°, respectively, while the corresponding ones approach 0.5° in **b** which seems therefore more symmetric. The angle between the C_{ipso} phenyl groups in **b** is wider than that in **a** by 2.9°.

As reported in Table 6, the Sn—C bond length is practically not affected, whereas the Sn—Cl and the Sn—N ones are slightly greater in presence of L^2 ($\Delta^* = 0.01$ Å for both). The same happens for the bite angles on Sn ($\Delta^* = 2.1°$) and on B ($\Delta^* = 1.0°$). Furthermore, comparing the ligands' coordination environments around Sn and B it may be found that: (i) for the angle N—Sn—B, $\Delta^* = 1.5°$, while for N—B—Sn, $\Delta^* = -0.5°$; (ii) for the angle N—N—Sn, $\Delta^* = -3.5°$ while for the N—N—B, $\Delta^* = 1.9°$. This, taken together with the above observations and with a decrease of the Sn···B distance ($\Delta^* = -0.06$ Å), may be approximately envisioned as a slight rotation of the μ-pyrazolate units in **b** (around their *pseudo*-C_5 axes) away from the Sn atom with respect to those in **a**. The Me(3)—C(3)—N(2) angle (the numbering scheme is that for Fig. 1) in **b** is also slightly greater (1.8°) than the corresponding one in $Fe(L^2)_2$.[10] This means that the overall steric hindrance attributable to Sn substituents is comparably (slightly) greater than three pyrazole groups since Fe^{2+} and Sn^{4+} have been attributed very similar ionic radii.

The present structure **c** ($SnCl_3 \cdot L^0$), together with that of $SnCl_3 \cdot L^2$,[7] offers the chance, as for the previous couple **a** and **b** of extending the comparison of the ligand's effects. In passing from L^0 to L^2 the Sn—N bond distances decreases ($\Delta^{**} = -0.036$ Å) while the Sn—Cl increases slightly. For the corresponding (mean) angles N—Sn—N and Cl—Sn—Cl, $\Delta^{**} = 2.5°$ and $-4.5°$, respectively. The presence of the methyl groups in position 3 in L^2 seems to force chlorine ligands away from tin with respect to the situation in L^0.

Mössbauer results

The average linewidths in Table 1, close to the minimum observable width[11] of 0.67 mm s^{-1}, point to the presence of only one distinguishable tin site in all the investigated compounds. This is in agreement with the crystallographically equivalent tin sites found in the above reported structures.

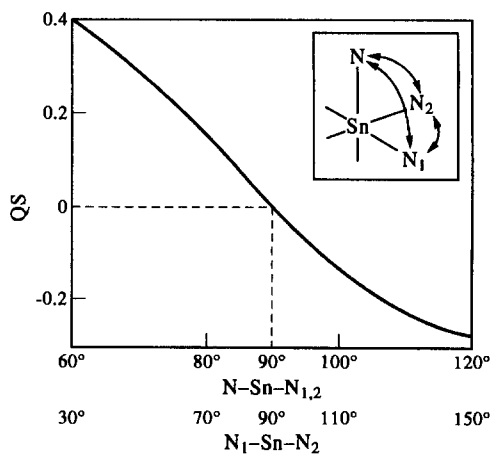

Fig. 4. Plot of the QS values *vs* the N—Sn—N angles, in degrees, for the inorganic compounds $SnCl_3 \cdot L$ **1–4**. (In the calculation the Cl ligands have been considered fixed and the N_1, N_2 pyrazolates variable in such a way that the angles $NSnN_1$, $NSnN_2$ and N_1SnN_2 have been considered simultaneously.)

For the inorganic series $SnCl_3 \cdot L$ (**1–4** in Table 1) the *s*-electron density at the tin nucleus and the small *p*-electronic asymmetry around the tin atom suggest for **2–4** a coordination geometry similar to that found in **1** or in **3**.[7]

In passing from **1** to **4** the progressive substitution on pyrazolate-type ligands (*cf* Fig. 1) determines a decrease of the electric quadrupole splitting and a more positive isomer shift (Table 1). Another concomitant effect of the substitution is that the mean N—Sn—N bond angle as well as the bond angle Cl—Sn—Cl, as evidence for $SnCl_3 \cdot L^0$ and $SnCl_3 \cdot L^2$ in Table 6, incline towards 90°, the value of the regular octahedral geometry. The quadrupole splitting decreases on going from **1** to **4** because the tin site becomes closer to the octahedral one. The increase of the *s*-electron density at the tin nucleus implies a decrease of the *s*-electron contribution in the hybridized bonds Sn—Cl, Sn—N and then more *regular* angular values in the SnN_3Cl_3 unity (Table 6).

The small quadrupole splitting, detected in the spectra of the compounds $SnCl_3 \cdot L$ (**1–4** in Table 1), depends mainly on their N—Sn—N angle owing to the very small contribution of the Cl ligands. This dependence is shown in Fig. 4 where the splitting has been calculated by point-charge approximation,[11,12] as a function of the three N—Sn—N angles. The plot shows that the quadrupole splitting is positive for an angle N—Sn—N smaller than 90°

For the compounds $RSnCl_2 \cdot L$ (**5–11**) and

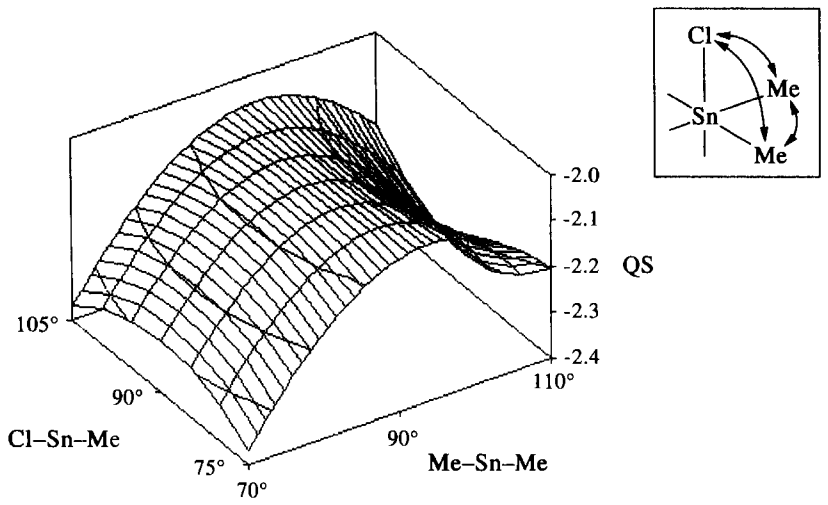

Fig. 5. Plot of the QS value *vs* the angles Me—Sn—Me and Cl—Sn—Me, in degrees for **20** $Me_2SnCl \cdot L^{0'}$. (In the octahedral geometry the N-tridentate ligand L has been considered undistorted since its very scarce contribution to the QS.)

$R_2SnCl \cdot L$ (**12–19** in Table 1) the magnitude of IS and QS parameters increases substantially with the number of Me or Ph groups. For these compounds in the *regular* octahedral geometry, the facial N-tridentate pyrazolate-type ligand L does not contribute to the magnitude of the principal components of the electric field gradient (e.f.g., *cf* footnote in Table 1). The e.f.g. components for the series $RSnCl_2 \cdot L$ and $R_2SnCl \cdot L$ are equal in magnitude but opposite in sign. The sign of their V_{zz} may be estimated by considering the relative electron donor power of the ligands. In the octahedral compounds $RSnCl_2 \cdot L$ more electronic charge is concentrated along the R—Sn—N axis in comparison with that in the plane defined by the axes N—Sn—Cl, giving a negative V_{zz}. Conversely in the octahedral compounds $R_2SnCl \cdot L$ less electronic charge is concentrated along the Cl—Sn—N axis, giving a positive V_{zz}. As a consequence, the quadrupole splitting is positive in the series $RSnCl_2 \cdot L$ and negative in the $R_2SnCl \cdot L$ one, because of the negative value of the ^{119m}Sn nuclear quadrupole moment.[11] The agreement between experimental and calculated splittings in Table 1 allows to attribute an octahedral geometry to the tin sites of the specimens **5–19**. This assignment is consistent with the crystal structures reported for **8**,[3b] **14**, **16** and $MeSnCl_2 \cdot L^3$.[8]

The effect of the progressive substitution on the pyrazolate-type ligands (Fig. 1) is less evidenced from the Mössbauer parameter of the organotin compounds (**5–19** in Table 1), than the inorganic ones, since the predominant inductive effect of the alkyl groups bonded to tin. On going from L^0 to L^1, L^2 or $L^{0'}$ in Table 1, the *s*-electron density at the tin nucleus increases slightly (showing that less *s*-electronic charge is delocalized in bonds) together with a slight decrease in the tin *p*-electron asymmetry (showing that the tin site becomes on the whole a little more regular). With reference to the present crystal structures for $Ph_2SnCl \cdot L^0$ and $Ph_2SnCl \cdot L^2$, the N—Sn—N and C—Sn—Cl bond angles incline towards 90°, causing *inter alia* a lengthening of the bonds Sn—Cl and Sn—N (Table 6). Conversely an increase of the C—Sn—C bond angles is observed since the steric hindrance of the

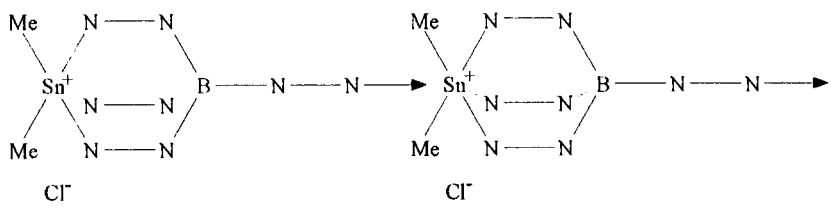

Fig. 6. Alternative octahedral coordination for **20** $Me_2SnCl \cdot L^{0'}$ with the N-tridentate ligand L and the N-ligand from the fourth pyrazolate.

Ph groups and the presence of substituents on L^2. The consequent large variation in the relative positions of the Ph planes is evidenced in Table 5.

The compound **20** $Me_2SnCl \cdot L^{0'}$ featuring the ligand $L^{0'}$, displays a splitting too large for a more or less distorted octahedral coordination, as shown in Fig. 5 where a plot of its calculated[12] quadrupole splitting *vs* the angles Me—Sn—Me and Cl—Sn—M is reported. In the same way the alternative octahedral coordination displayed in Fig. 6, with one facial N-tridentate ligand and one N-monodentate ligand coming from the fourth pyrazolate, is ruled out since the splitting for this polymeric species is too small.

If the tetrakis(pyrazolyl)borate in **20**, $Me_2SnCl \cdot L^{0'}$, acts as N-bidentate in a trigonal–bipyramidal coordinate geometry, among the five possible isomers, only that with equatorial methyls has a calculated splitting ($+2.91$ mm s^{-1}) close to the observed one.

In conclusion a distorted octahedral geometry on (organo)tin(IV) polypyrazoly-1-borates $R_nSnCl_{3-n} \cdot L$ with a facial N-tridentate ligand appears to be the rule for $n = 0$ or 1, while for $n = 2$ and $L = L^{0'}$ a lowering of the coordination number to 5 with a bidentate ligand might be possible. This is expected in that the ligand $L^{0'}$, more readily than the others in the family, may act as bidentate and consequently favour fluxionality.[4a,13] It is more likely with the Me_2SnCl^+ moiety which is a better Lewis acid than Ph_2SnCl^+.

Acknowledgements—Financial support from the CNR-Rome, MURST and NATO (CRG 920179 to S.C.) is gratefully acknowledged.

REFERENCES

1. (a) S. Trofimenko, *Prog. Inorg. Chem.* 1986, **34**, 115; (b) K. Niedenzu and S. Trofimenko, *Topics Curr. Chem.* 1986, **131**, 1; (c) S. Trofimenko, *Chem. Rev.* 1993, **93**, 943; *Chem. Rev.* 1972, **72**, 497; (d) K. Niedenzu, H. Nöth, J. Serwatowska and J. Serwatowski, *Inorg. Chem.* 1991, **30**, 3249; (e) C. H. Dungan, W. Maringgele, A. Meller, K. Niedenzu, H. Nöth, J. Serwatowska and J. Serwatowski, *Inorg. Chem.* 1991, **30**, 4799; (f) A. Looney, *Polyhedron* 1990, **9**, 265; (g) M. A. J. Moss and C. J. Jones, *Polyhedron* 1990, **9**, 1119; (h) S. Trofimenko, J. C. Calabrese and J. S. Thompson, *Angew. Chem., Int. Ed. Engl.* 1989, **28**, 205.
2. (a) D. L. Reger, S. J. Knox, M. F. Huff, A. L. Rheigold and B. S. Haggerty, *Inorg. Chem.* 1991, **30**, 1754; (b) M. N. Hansen, K. Niedenzu, J. Serwatowska, J. Servatowski and K. Woodrum, *Inorg. Chem.* 1991, **30**, 866; (c) D. L. Reger, S. J. Knox, A. L. Rheigold and B. S. Haggerty, *Organometallics* 1990, **9**, 2581; (d) D. L. Reger, S. J. Knox and L. Lebioda, *Organometallics* 1990, **9**, 2218; (e) M. Di Vaira and F. Mani, *J. Chem. Soc., Dalton Trans.* 1990, **1**, 191; (f) A. Duatti, F. Tisato, F. Refosco, U. Mazzi and M. Nicolini, *Inorg. Chem.* 1989, **28**, 4564; (g) R. A. Kresinski, T. A. Hamor, L. Isam, C. J. Jones and J. A. McCleverty, *Polyhedron* 1989, **8**, 845.
3. (a) G. Gioia Lobbia, F. Bonati, P. Cecchi, A. Cingolani and A. Lorenzotti, *J. Organomet. Chem.* 1989, **378**, 139; (b) G. Gioia Lobbia, S. Calogero, B. Bovio and P. Cecchi, *J. Organomet. Chem.* 1992, **440**, 27; (c) G. Gioia Lobbia, F. Bonati, P. Cecchi, A. Lorenzotti and C. Pettinari, *J. Organomet. Chem.* 1991, **403**, 317; (d) G. Gioia Lobbia, F. Bonati, P. Cecchi and D. Leonesi, *J. Organomet. Chem.* 1990, **391**, 155.
4. (a) G. Gioia Lobbia, F. Bonati, P. Cecchi and C. Pettinari, *Gazz. Chim. Ital.* 1991, **121**, 355; (b) G. Gioia Lobbia, P. Cecchi, F. Bonati and G. Rafaini, *Synth. React. Inorg. Metal-Org. Chem.* 1992, **22**, 775; (c) G. Gioia Lobbia, F. Cecchi, S. Bartolini, C. Pettinari and A. Cingolani, *Gazz. Chim. Ital.* 1993, **123**, 641.
5. G. Gioia Lobbia, S. Zamponi, R. Marassi, M. Berrettoni, S. Stizza and P. Cecchi, *Gazz. Chim. Ital.* 1993, **13**, 389.
6. S. A. A. Zaidi, A. A. Hashmi, K. S. Siddiqi, *J. Chem. Res. (S)* 1988, 410.
7. O. S. Jung, J. H. Jeong and Y. S. Sohn, *J. Organomet. Chem.* 1990, **399**, 235.
8. G. Gioia Lobbia, P. Cecchi, R. Spagna, M. Colapietro, A. Pifferi and C. Pettinari, *J. Organomet. Chem.* 1995, **485**, 45.
9. D. Collison, D. R. Eardley, F. E. Mabbs, K. Rigby, M. A. Bruk, J. H. Enemark and P. A. Vexler, *J. Chem. Soc., Dalton Trans.* 1994, 1003.
10. J. D. Oliver, D. F. Mullica, B. B. Hutchinson and W. O. Milligan, *Inorg. Chem.* 1980, **19**, 165.
11. R. V. Parish, in *Mössbauer Spectroscopy Applied to Inorganic Chemistry* (Edited by G. J. Long), Vol. I, p. 527. Plenum Press, New York (1984).
12. S. Calogero and C. D'Arrigo, *Quantum Chemistry Program Exchange, Newsletters* 1978, **63**, 46, n. 367.
13. S. Aime, R. Gobetto, G. Digilio, G. Gioia Lobbia and P. Cecchi, *Polyhedron* 1994, **18**, 2695.